 doi:10.20944/preprints202012.0192.v1

Article

Numerical Method for Coupled Nonlinear Schrödinger Equations in Few Mode Fiber

Airat Zh. Sakhabutdinov [1,*], Vladimir I. Anfinogentov [1], Oleg G. Morozov [1], Vladimir A. Burdin [2], Anton V. Bourdine [2,3], Artem A. Kuznetsov [1], Dmitry V. Ivanov [4], Vladimir A. Ivanov [4], Maria I. Ryabova [4], and Vladimir V. Ovchinnikov [4]

[1] Department of Radiophotonics and Microwave Theory, Kazan National Research State University named after A.N. Tupolev-KAI, 31/7, Karl Marx street, Kazan, Rep. Tatarstan 420111, Russia; KazanBoy@yandex.ru (A.Zh.S.); VIAnfinogentov@kai.ru (V.I.A.); microoil@mail.ru (O.G.M.); AAKuznetsov@kai.ru (A.A.K.)

[2] Department of Communication Lines, Povozhskiy State University of Telecommunications and Informatics, 23, Lev Tolstoy street, Samara 443010, Russia; burdin@psati.ru (V.A.B.); bourdine@yandex.ru (A.V.B.)

[3] JSC "Scientific Production Association State Optical Institute Named after Vavilov S.I.", 36/1, Babushkin street, Saint Petersburg 192171, Russia; (A.V.B.)

[4] Volga State University of Technology, 3, Lenin Sq., Yoshkar-Ola, Rep. Mari El 424000, Russia; IvanovDV@volgatech.net (D.V.I.); IvanovVA@volgatech.net (V.A.I.); RyabovaMI@volgatech.net (M.I.R.); OvchinnikovVV@volgatech.net (V.V.O.);

* Correspondence: azhsakhabutdinov@kai.ru; Tel.: +7-987-290-1864

Abstract: This paper discusses approaches to the numerical integration of the coupled nonlinear Schrödinger equations system in case of few-mode wave propagation. The wave propagation assumes the propagation of up to nine modes of light in an optical fiber. In this case, the light propagation is described by the non-linear coupled Schrödinger equation system, where propagation of each mode is described by own Schrödinger equation with other modes interactions. In this case, the non-linear coupled Schrödinger equation system solving becomes increasingly complex, because each mode affects the propagation of other modes. The suggested solution is based on the direct numerical integration approach, which is based on a finite-difference integration scheme. The well-known explicit finite-difference integration scheme approach fails, due to the non-stability of the computing scheme. Due to this fact, the combined explicit/implicit finite-difference integration scheme, based on the implicit Crank–Nicolson finite-difference scheme, is used. It allows ensuring the stability of the computing scheme. Moreover, this approach allows separating the whole equation system on the independent equation system for each wave mode at each integration step. Additionally, the algorithm of numerical solution refining at each step and the integration method with automatic integration step selection are used. The suggested approach has performance gains (or resolutions) up to three or more orders of magnitude in comparison with the split-step Fourier method due to the fact that there is no need to produce direct and inverse Fourier transforms at each integration step. The main advantage of the proposed method is the ability to calculate the propagation of an arbitrary number of modes in the fiber.

Keywords: nonlinear Schrödinger equation system; few-mode propagation; Kerr effect; Raman scattering; dispersion; implicit/explicit Crank–Nicolson scheme; pulse chirping, second-order dispersion, third-order dispersion, chirp pulse, optical pulse compression, pulse collapse

1. Introduction

This article is a continuation of our previous work [1], where we suggest the original solution of coupled nonlinear Schrödinger equations for simulation of ultra-short optical pulse propagation in birefringent fibers. The introduction of our previous work [1] completely reveals the reasons and importance and the necessity of the problem formulation. It is necessary to emphasize, that pulse propagation in fibers with abnormal dispersion is an important investigation theme because the

Preprints (www.preprints.org) | NOT PEER-REVIEWED | Posted: 8 December 2020 doi:10.20944/preprints202012.0192.v1

femtosecond lasers have a strong position in the industrial [2–5]. The special optical fibers are developed for high-power ultrashort pulses [6–7] transmission with special attention to polarization maintaining fibers. The negative role of chromatic dispersion appears with an increase of the length of the optical fiber communication line. The physical reason for dispersion is the frequency dependence of the phase velocity or phase delay during propagation of electromagnetic waves in the medium. This leads to a violation of the phase vectors in the wave package. When these negative effects are studied, only envelope distortion is usually considered. However, phase distortions are also important for the certain class of problems. For example, the problem of chirping during the propagation of an optical signal in an optical fiber with nonlinear dispersion is one of them.

The first part of the work is devoted to computing method of complex envelop calculation, the second part of the work is devoted to the phase velocity or phase delay calculation during the propagation of optical waves in the fibers.

2. Computing Method for Complex Envelopes of the Optical Wave Calculation

2.1 Coupled Nonlinear Schrödinger Equation System for Few Modes in Dimensionless Form

The evolution of optical wave in a fiber can be described by the coupled nonlinear Schrödinger equation system:

$$\begin{cases} \dfrac{\partial W^{(i)}}{\partial z} = -\dfrac{\alpha^{(i)}}{2} W^{(i)} - \beta_1^{(i)} \dfrac{\partial W^{(i)}}{\partial t} - j\dfrac{\beta_2^{(i)}}{2} \dfrac{\partial^2 W^{(i)}}{\partial t^2} + \dfrac{\beta_3^{(i)}}{6} \dfrac{\partial^3 W^{(i)}}{\partial t^3} + \\ + j\gamma^{(i)} W^{(i)} \sum_{m=1}^{M} C_{i,m} \left| W^{(m)} \right|^2 - \dfrac{\gamma^{(i)}}{\omega_0^{(i)}} \sum_{m=1}^{M} B_{i,m} \dfrac{\partial}{\partial t} \left(\left| W^{(m)} \right|^2 W^{(i)} \right) - j\gamma^{(i)} T_R W^{(i)} \sum_{m=1}^{M} B_{i,m} \dfrac{\partial}{\partial t} \left(\left| W^{(m)} \right|^2 \right), \\ i = \overline{1,M}, \end{cases} \quad (1)$$

with the initial and boundary conditions for each propagation mode:

$$W^{(i)}(z,0) = 0,\ \frac{\partial W^{(i)}(z,0)}{\partial t} = 0,\ W^{(i)}(z,T_N) = 0, \forall z \in [0,L],\ W^{(i)}(0,t) = f^{(i)}(t),\ 0 \le t \le T_N,\ i = \overline{1,M}, \quad (2)$$

The definitions are used in Equations (1)–(2): W_i—the complex envelope of the optical wave of the i-th mode, $\alpha^{(i)}$—attenuation coefficient of the i-th mode; $\beta^{(i)}{}_1$, $\beta^{(i)}{}_2$, $\beta^{(i)}{}_3$—the first, second and third order dispersion parameters of the i-th mode respectively; $\gamma^{(i)}$—nonlinearity parameter for the i-th mode; $C_{i,m}$, $B_{i,m}$—coupling coefficients between the i-th and m-th modes; T_R—Raman scattering parameter; $\omega^{(i)}{}_0$—angular frequency of the i-th mode; z—coordinate along an optical fiber; t—time, j – imaginary one, T_N—final time, and $f^{(i)}(t)$ – known functions at the initial time.

To transfer Equation (1) into dimensionless form, the specific values of the process are used, namely L— length, T_N— time, and P—power, by relations:

$$\xi = z/L,\ \tau = t/T_N,\ x^{(i)} = W^{(i)}/\sqrt{P}, \quad (3)$$

Replacement of Equation (3) into Equation (1) transforms it into dimensionless form:

$$\left\{ \frac{\partial x^{(i)}}{\partial \xi} = -\left[a^{(i)} + \Phi 1^{(i)} \right] \cdot x^{(i)} - \left[b_1^{(i)} + \Phi 2^{(i)} \right] \cdot \frac{\partial x^{(i)}}{\partial \tau} - jb_2^{(i)} \frac{\partial^2 x^{(i)}}{\partial \tau^2} + b_3^{(i)} \frac{\partial^3 x^{(i)}}{\partial \tau^3},\ i = \overline{1,M}, \right. \quad (4)$$

where the dimensionless coefficients:

$$a^{(i)} = \frac{\alpha^{(i)} L}{2},\ b_1^{(i)} = \beta_1^{(i)} \frac{L}{T},\ b_2^{(i)} = \frac{\beta_2^{(i)}}{2} \frac{L}{T^2},\ b_3^{(i)} = \frac{\beta_3^{(i)}}{6} \frac{L}{T^3},\ u^{(i)} = \gamma^{(i)} LP,\ v^{(i)} = \frac{u^{(i)}}{\omega_0 T}, w^{(i)} = u^{(i)} \frac{T_R}{T_N}, \quad (5)$$

and the definitions for non-linear component:

Preprints (www.preprints.org) | NOT PEER-REVIEWED | Posted: 8 December 2020 doi:10.20944/preprints202012.0192.v1

$$\Phi 1^{(i)} = (v^{(i)} + jw^{(i)}) \cdot \sum_{m=1}^{M} B_{i,m} \frac{\partial}{\partial \tau} \left(\left| x^{(m)} \right|^2 \right) - ju^{(i)} \sum_{m=1}^{M} C_{i,m} \left| x^{(m)} \right|^2, \quad \Phi 2^{(i)} = v^{(i)} \sum_{m=1}^{M} B_{i,m} \left| x^{(m)} \right|^2, \tag{6}$$

are used.

The Equation (1) is specially separated on linear and nonlinear terms, it allows us to realize the numerical integration algorithm based on computing scheme, where all linear terms are written in implicit and all nonlinear terms are written in explicit finite-difference form.

2.2. The Finite-Difference Scheme and Computing Scheme

The Equation system (4) can be rewritten in the simple form where definitions $F^{(i)}(\mathbf{x})$ are used to denote the right parts of Equation (4):

$$\left\{ \frac{\partial x^{(i)}}{\partial \xi} = F^{(i)}, \; i = \overline{1, M} \right. . \tag{7}$$

The finite-difference equivalences for Equation (7), according to [1], have the form:

$$\left\{ \frac{\left(x_{k+1,n}^{(i)} + x_{k+1,n-1}^{(i)} \right) - \left(x_{k,n}^{(i)} + x_{k,n-1}^{(i)} \right)}{2\Delta\xi} = \theta \cdot F_{k+1,n-1/2}^{(i)} + (1-\theta) \cdot F_{k,n-1/2}^{(i)}, \; i = \overline{1, M}, \; n = \overline{3, N-1}, \; k = \overline{1, K} \right. , \tag{8}$$

where bottom index k is used to denote the mesh points along the length $\xi_k = \Delta\xi \cdot (k-1)$ and n is used to denote the dimensionless time mesh points $\tau_n = \Delta\tau \cdot (n-1)$. The dimensionless parameter θ allows to attribute the value of right part of Equation (8) to an arbitrary mesh point with fractional indexes $(k + \theta, n - ½)$. The parameter $\theta \in [0, 1]$, defines the explicit $\theta = 0$ or implicit $\theta \in (0, 1]$ finite-difference computing scheme. The recommendation for θ parameter choosing was given in [1]. There it was approved that $\theta = ½$, that leads to stable and reasonable results.

All variables with the k-index in Equation (8) are known as well as all variables with the $(k + 1)$ indexes are known at n equal to 0, 1, 2 and N from Equation (2). The values of $F^{(i)}$ are attributed to middleware virtual mesh points between $(k+ \theta, n - ½)$.

The nonlinearity in $\Phi 1^{(i)}$ and $\Phi 2^{(i)}$, and a third-order partial derivative by time in Equation (4), require to use the modification of Crank–Nicolson computing scheme [1, 16]. The main idea of it is to write all linear terms in implicit form, and all nonlinear terms in explicit form. So, we separate the $F^{(i)}$ on the sum of linear and nonlinear terms:

$$F_{k,n-1/2}^{(i)} = L_{k,n-1/2}^{(i)} + N_{k,n-1/2}^{(i)}, \tag{9}$$

with the definitions for linear $L^{(i)}$ and non-linear $N^{(i)}$ terms at k-layer:

$$\begin{gathered} L_{k,n-1/2}^{(i)} = -a x_{k,n-1/2}^{(i)} - b_1^{(i)} \left(\frac{\partial x^{(i)}}{\partial \tau} \right)_{k,n-1/2} - j b_2^{(i)} \left(\frac{\partial^2 x^{(i)}}{\partial \tau^2} \right)_{n-1/2,k} + b_3^{(i)} \left(\frac{\partial^3 x^{(i)}}{\partial \tau^3} \right)_{k,n-1/2}, \\ N_{k,n-1/2}^{(i)} = -\Phi 1_{k,n-1/2}^{(i)} x_{k,n-1/2}^{(i)} - \Phi 2_{k,n-1/2}^{(i)} \left(\frac{\partial x^{(i)}}{\partial \tau} \right)_{k,n-1/2} \end{gathered} \tag{10}$$

For the definition of the linear terms $L^{(i)}$ on $(k + 1)$-th layer, it is enough to replace k on $(k + 1)$ in Equation (10). For nonlinear terms on $(k + 1)$-th layer, it is necessary to use explicit finite-difference definition:

$$N_{k+1,n-1/2}^{(i)} = -\Phi 1_{k,n-1/2}^{(i)} x_{k+1,n-1/2}^{(i)} - \Phi 2_{k,n-1/2}^{(i)} \left(\frac{\partial x^{(i)}}{\partial \tau} \right)_{k+1,n-1/2}. \tag{11}$$

Hence, the explicit form in Equation (8) is used only for $\Phi 1^{(i)}$ and $\Phi 2^{(i)}$, while the implicit form is used for the linear terms. The nonlinear terms $\Phi 1^{(i)}$ and $\Phi 2^{(i)}$ in virtual mesh point $(k, n - ½)$ are written as:

Preprints (www.preprints.org) | NOT PEER-REVIEWED | Posted: 8 December 2020 doi:10.20944/preprints202012.0192.v1

$$\Phi 1^{(i)}_{k,n-1/2} = -\frac{ju^{(i)}}{2}\sum_{m=1}^{M} C_{i,m}\left(\left|x^{(m)}_{k,n}\right|^2 + \left|x^{(m)}_{k,n-1}\right|^2\right) + \frac{v^{(i)} + jw^{(i)}}{\Delta\tau}\sum_{m=1}^{M} B_{i,m}\left(\left|x^{(m)}_{k,n}\right|^2 - \left|x^{(m)}_{k,n-1}\right|^2\right),$$
$$\Phi 2^{(i)}_{k,n-1/2} = \frac{v^{(i)}}{2}\sum_{m=1}^{M} B_{i,m}\left(\left|x^{(m)}_{k,n}\right|^2 + \left|x^{(m)}_{k,n-1}\right|^2\right). \quad (12)$$

The desired function values in mesh point (k, n – ½) are written as a half of its sum in neighbor mesh points. The partial derivative from desired functions on time in the same mesh point are written as central finite-differences with second-order accuracy. It gives the linear equation system for each mode at each integration step:

$$\begin{cases} \frac{x^{(i)}_{k+1,n} + x^{(i)}_{k+1,n-1}}{2\cdot\Delta\xi\cdot\theta} + \frac{a + \Phi 1^{(i)}_{k,n-1/2}}{2}\left(x^{(i)}_{k+1,n} + x^{(i)}_{k+1,n-1}\right) + \frac{b^{(i)}_1 + \Phi 2^{(i)}_{k,n-1/2}}{\Delta\tau}\left(x^{(i)}_{k+1,n} - x^{(i)}_{k+1,n-1}\right) + \\ + \frac{jb^{(i)}_2}{2\Delta\tau^2}\left(x^{(i)}_{k+1,n+1} - x^{(i)}_{k+1,n} - x^{(i)}_{k+1,n-1} + x^{(i)}_{k+1,n-2}\right) - \frac{b^{(i)}_3}{\Delta\tau^3}\left(x^{(i)}_{k+1,n+1} - 3x^{(i)}_{k+1,n} + 3x^{(i)}_{k+1,n-1} - x^{(i)}_{k+1,n-2}\right) = \\ = \frac{x^{(i)}_{k,n} + x^{(i)}_{k,n-1}}{2\cdot\Delta\xi\cdot\theta} + \frac{(1-\theta)}{\theta}\left(L^{(i)}_{k,n-1/2} + N^{(i)}_{k,n-1/2}\right) \\ n = \overline{2, N-1},\ i = \overline{1, M} \end{cases} \quad (13)$$

It is very important to note, that the linear Equation system (13) for i-th mode depends only on $x^{(i)}_{k+1,n}$ unknowns and does not depend on unknowns from other wave modes. It allows solving the linear equation system for the each i-th mode independently. The index n for each linear equation system for i-th mode begins from 2 up to the N – 1, because the values of $x_{k+1,1}$, $x_{k+1,2}$, and $x_{k+1,N}$ are known due to the Equation (2).

It should be especially noted that the Equation system (13) breaks down into M independent line equation systems, relative to mesh node variables $x^{(i)}_{k+1,n}$ (where n begins from 3 and increases to N–1). Each equation system can be solved separately. These linear equation systems have four-diagonal matrix form, where in addition to main diagonal, there are one "upper" and two "sub" diagonals. We use the modification of Thomas tridiagonal algorithm, which allows transforming the four-diagonal matrix to the triangular form. The refining solution algorithm is used at each integration step. The explicit nonlinear terms determination (from previous k-th integration layer) makes its contribution to the inaccuracy of new (k + 1)-th layer values calculation. The main idea of the refining algorithm is in the iterative process organization at each integration step, which corrects the explicit form of nonlinear terms [1].

2.3. The Ultra-Short Pulse Evolution in Fiber

The ultra-short pulse evolution in fiber with third-order dispersion and Raman scattering is described by complete coupled nonlinear Schrödinger equations system. The values from [8–15], which were used in their experiment, were taken as: $\alpha^{(1)} = \alpha^{(2)} = 0.2$ dB·m/km, $\beta^{(1)} = 4.294\times10^{-9}$ s/m, $\beta^{(2)}{}_1 = 4.290\times10^{-9}$ s/m, $\beta^{(1)}{}_2 = 3.600\times10^{-26}$ s²/m, $\beta^{(2)}{}_2 = 3.250\times10^{-26}$ s²/m, $\beta^{(1)}{}_3 = \beta^{(2)} = 2.750\times10^{-41}$ s³/m, $\gamma^{(1)} = \gamma^{(2)} = 3.600\times10^{-2}$ (m·W)$^{-1}$, $T_R = 4.000\times10^{-15}$ s, $\omega^{(1)}{}_0 = \omega^{(2)}{}_0 = 2.3612\times10^{-15}$ s^{-1} (wavelength 798 nm). The single chirped Gauss pulse is in the input fiber end (chirp C = –0.4579), pulse duration is 12 fs, with maximum power $P = 1.75\times10^5$ W. The pulse form is described as:

$$f(t) = A\cdot\exp\left(-\frac{(1 - j\cdot C)(t - T_N)^2}{2\cdot\tau^2}\right). \quad (14)$$

The number of mesh points along dimensionless time was chosen as 20,000; approximately 720,000 integration steps were made along dimensionless time with initial time step $\Delta\xi = 1\cdot10^{-4}$ d.u. Besides, the automatic integration step correction algorithm was included. It allowed to calculate the pulse evolution length up to ~2.5 mm. The maximum error for iteration process was chosen as 10^{-30} d.u. All calculations were made in a processor with double precision and 64-bit architecture.

Preprints (www.preprints.org) | NOT PEER-REVIEWED | Posted: 8 December 2020 doi:10.20944/preprints202012.0192.v1

The pulse evolution according to computing results is shown in Figure 1 by the red line, in compare the experimental results [8–15] are shown by the blue line.

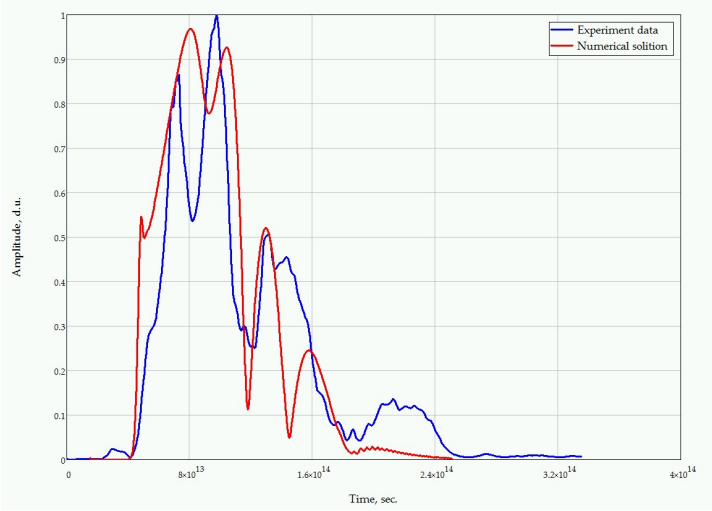

Figure 1. The pulse form evolution in fiber. Numerical calculation results of coupled nonlinear Schrödinger equations system are marked by the red line and the experimental results obtained by [8–15] are marked by the blue line.

The numerical result (red line in Figure 1) is in good matching with experimental result (blue line in Figure 1). It excellently confirms that the suggested method is effective and can be used for solving the similar nonlinear tasks.

3. The Phase Velocity or Phase Delay Calculation during the Wave Propagation

Recently, the channel model, based on equivalence principle [17-19], is used for description of propagation of wave packages in media. According to this model, the task of wave package propagation is replaced by the task of wave package passing through line system with frequency $H(j\omega)$ and $h(\tau)$ impulse characteristics:

$$\begin{gathered} H(j\omega,L)=\left|H(j\omega,L)\right|\exp\left[-j\varphi(\varpi+\Omega,L)\right],\ \varphi(\omega,L)=-Arg\left(H\left(j\omega,L\right)\right), \\ H(j\omega,L)=F\left[h(\tau,L)\right],\ h(\tau,L)=F^{-1}\left[H(j\omega,L)\right], \end{gathered} \tag{15}$$

where $\varphi(\omega)$ is phase incursion in media or phase-frequency characteristic of the line system, where the frequency set of the package ω can be presented as the sum of average ϖ and difference Ω package frequencies as $\omega = \varpi + \Omega$. The $F[]$ and $F^{-1}[]$ denote direct and inverse Fourier transform operator.

It is convenient to use the expression of time delays instead of velocities of propagation while studying the dispersion. Therefore, the phase delay τ_p and group delay τ_g (fast time) terms are involved into consideration, which are defined from phase-frequency characteristics of the system [20]:

$$\tau_p(\omega,L)=\frac{\varphi(\omega,L)}{\omega},\quad \tau_g(\omega,L)=\frac{d\varphi(\omega,L)}{d\omega}. \tag{16}$$

The minus sign "–" ahead the phase $\varphi(\omega, L)$ of frequency characteristic in Equation (15) is introduced in order to the derivative of phase defines the phase delay. Group delay is a differential characteristic of phase incursion in the media (in the neighborhood of the selected frequency), and phase delay is an integrated characteristic.

The most common approach in the investigation of dispersion is related to the differential characteristic definition, where frequency characteristic covers the frequency range Ω_{ch} with average frequency ϖ, and amplitude-frequency and phase-frequency characteristics (Equation (15)) are

Preprints (www.preprints.org) | NOT PEER-REVIEWED | Posted: 8 December 2020 doi:10.20944/preprints202012.0192.v1

presented by Taylor power series of deferential frequencies $(\omega - \varpi) = \Omega$ at the ϖ average frequency point:

$$H(\varpi+\Omega)\approx H(\varpi)\equiv const\ . \tag{17}$$

$$\varphi(\varpi+\Omega)\approx\varphi(\varpi)+\varphi'(\varpi)\cdot\Omega+\frac{1}{2}\varphi''(\varpi)\cdot\Omega^2+\frac{1}{6}\varphi'''(\varpi)\cdot\Omega^3+o(\Omega^4),\ \ \forall\Omega\in\left[-\Omega_{ch}/2,\Omega_{ch}/2\right] \tag{18}$$

For a homogeneous medium, among which there is optical fiber, the phase-frequency characteristic is related to the refractive index of a fiber $n(\omega)$ and fiber length L by the relation:

$$\varphi(\omega,L)=\frac{L}{c}\omega\cdot n(\omega) \tag{19}$$

The coefficients at frequencies in the Taylor power series of phase-frequency characteristic Equation (18) are the parameters of phase dispersion of appropriate order. Thus, the dispersion parameters are evolving with increasing the length L in dispersal systems. When some critical length is achieved, the dispersal distortions occur due to the non-linear terms effects on phase-frequency characteristic.

It is convenient to use the group phase delay as a function of frequency for phase dispersion analysis in the channel model:

$$\tau_g(\varpi+\Omega,L)=\frac{d\varphi(\omega,L)}{d\omega}=\tau_g(\varpi,L)+\tau_g'(\varpi,L)\cdot\Omega+\frac{1}{2}\tau_g''(\varpi,L)\cdot\Omega^2+o(\Omega^3). \tag{20}$$

The $\varphi''(\varpi, L) = \tau'_g(\varpi, L)$ parameter is commonly referred to as Group-Delay Dispersion (GDD), and the $\tau''_g(\varpi, L) = \varphi'''(\varpi, L)$ = TOD parameter is commonly referred to as Third-Oder Dispersion (TOD).

The complex frequency characteristic is proportional to non-zero function in frequency channel in case of phase incursion describing by the Equation (18) without third-order dispersion $(\varphi'''(\varpi,L) = 0)$:

$$H(j(\varpi+\Omega),L)\ \propto\ \exp\left[-j\frac{\varphi''(\varpi,L)}{2}\Omega^2\right]. \tag{21}$$

The chirplet with rectangular duration window T_{ef} in time domain corresponds to the function $\exp(-j\varphi''(\varpi, L)\Omega^2/2)$ in frequency domain at $\Omega_{ch}T_{ef} >> 1$ (where $T_{ef} \approx \varphi''(\varpi,L)\cdot\Omega_{ch}$), according to Fourier transform property:

$$h(\varpi,\tau,L)\ \propto\ \exp\left[j\frac{\upsilon(\varpi,L)}{2}\tau^2\right],\ \text{where}\ \ \upsilon(\varpi,L)=1/\varphi''(\varpi,L). \tag{22}$$

The chirplets with rectangular duration window are shown in the Figure 1 in the case when $\Omega_{ch}T_{ef} >> 1$. The low frequencies are shown by the red lines, and high frequencies are shown by the blue lines.

The picture in Figure 2 shows that second-order frequency dispersion leads to chirping of impulse characteristic by fast time. In the case of normal dispersion, the low frequencies outrun high frequencies and the chirp sign is positive $(\upsilon(\varpi, L) > 0)$, in the case of anomalous dispersion, the chirp sign is negative $(\upsilon(\varpi, L) < 0)$.

The analytical solution for chirplet with rectangular window in case of second-order dispersion has the form [20]:

$$h(\varpi,\tau,L)=\frac{H(\varpi,L)\exp(j\theta)}{\sqrt{2\pi\varphi''(\varpi,L)}}\left[\left(C(z_2)-C(z_1)\right)-i\left(S(z_2)-S(z_1)\right)\right]\approx\frac{H(\varpi,L)\exp\left(j(\theta-\pi/4)\right)}{2\sqrt{\pi\varphi''(\varpi,L)}} \tag{23}$$

where $C(z)$, $S(z)$ is Fresnel integrals , θ_0 = const , and:

Preprints (www.preprints.org) | NOT PEER-REVIEWED | Posted: 8 December 2020 doi:10.20944/preprints202012.0192.v1

$$z_1=\frac{\tau-\tau_g(\varpi,L)}{\sqrt{\pi\varphi''(\varpi,L)}}-\Omega_{ch}\sqrt{\varphi''(\varpi,L)/\pi}\,,\ z_2=\frac{\tau-\tau_g(\varpi,L)}{\sqrt{\pi\varphi''(\varpi,L)}},\quad \theta=\theta_0+\varpi(\tau-\tau_g(\varpi,L))+\frac{1}{2\varphi''(\varpi,L)}(\tau-\tau_g(\varpi,L))^2 \tag{24}$$

The rough equilibrium in Equation (23) is true at $\Omega_{ch}T_{ef} \gg 1$ and other than zero at delays $\tau \in [\tau_g(\varpi, L) - T_{ef}/2; \tau_g(\varpi, L) + T_{ef}/2)$.

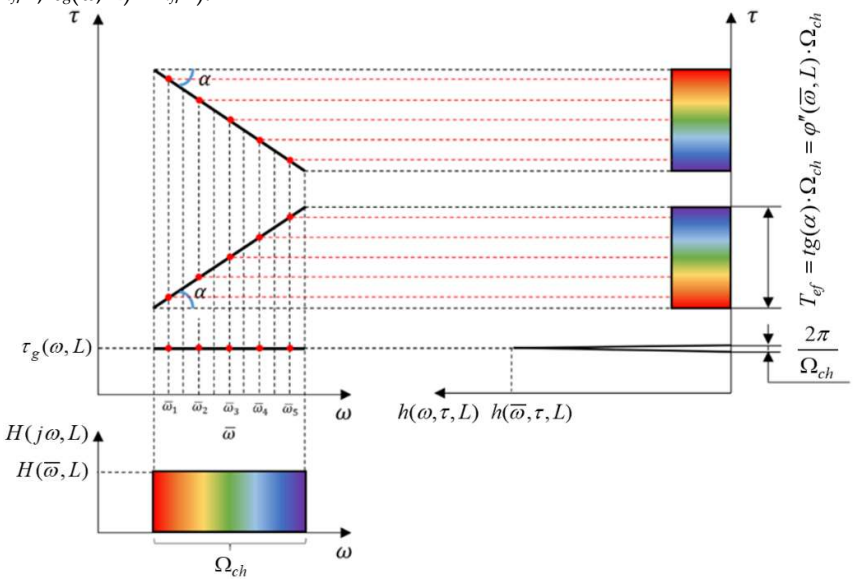

Figure 2. The Chirplets with rectangular duration window in the case of normal and anomalous dispersions and its pulse characteristics at soliton mode during the propagation in the medium.

According to Equation (23), the pulse characteristic of the channel is a chirplet by fast time τ, that is second-order dispersion leads to chirping of impulse characteristic. The rate of the frequency changing in the chirplet is positive for normal dispersion and is negative for anomalous dispersion.

The chirp effect can lead to the compactification of linear modulated pulse in the medium with second-order dispersion. Optical pulse with Gauss form with line frequency modulation $\omega = \varpi + \omega' t$, as well as frequency characteristic of communication line, has phase with quadratic dependence from frequency $\varphi''(\varpi, L)\Omega^2/2$. Therefore, if the condition $\Omega^2/2\omega' + \varphi''(\varpi, L_a)\cdot\Omega^2/2 = 0$ is fulfilled at given communication line length $L = L_a$, the linear frequency modulated pulse is matched with dispersal radio channel and it compresses over the fast time. This condition can be rewritten in the form $\omega'\cdot\varphi''(\varpi, L_a) = -1$. It means that the submitted derivatives must be reciprocal in magnitude and opposite in signs. Thus, for fiber with normal dispersion $\varphi''(\varpi, L) > 0$ the frequency changing rate of the optical pulse must be negative $\omega' < 0$, while for the fiber with anomalous dispersion it must have a positive sign.

With the increase of the line length at different signs of derivatives the dispersion parameter $\varphi''(\varpi, L)$ increases by the module. Therefore, the correlation with line frequency-modulated pulse with dispersion in optical fiber is fulfilled for certain line length $L = L_a$.

The computing experiments for the effect were carried out, considering that the phase-frequency characteristic of the channel, given as the line system, is dimensionless. Therefore, the terms in Equation (18) are also dimensionless; it allows to present each term as the product of dimensionless values.

Let us get the coherence range of the channel Ω_{c2} with second-order dispersion from the equivalence $|\varphi''(\varpi, L)(\Omega_{c2}/2)^2| = 1$, choosing as the line length $L = L_{e2}$ the value, for which $\Omega_{c2} = \Omega_{ch}$. Therefore, the communication line length can be evaluated by the relation:

$$L_{e2}=\frac{2c}{(\varpi\cdot n(\varpi))''}\cdot\left(\frac{2}{\Omega_{c2}}\right)^2,\ \text{where}\ \ \Omega_{c2}=2\cdot\sqrt{2/|\varphi''(\varpi,L)|} \tag{25}$$

Preprints (www.preprints.org) | NOT PEER-REVIEWED | Posted: 8 December 2020 doi:10.20944/preprints202012.0192.v1

Thus, it gives the equations for dimensionless values (dimensionless length $m = L/L_{e2}$, dimensionless second-order dispersion coefficient, and dimensionless frequency $\eta = 2\Omega/\Omega_{ch}$), where second-order dispersion is described by relation:

$$\frac{1}{2}\varphi''(\varpi, L)\cdot\Omega^2 = m\cdot\eta \tag{26}$$

The computing results of the compression of line frequency-modulated pulse with the Gauss form in the fiber with second-order dispersion in dimensionless values are presented in Figure 3. The real part of its envelope is given in the form, where its duration defines the frequency range of the channel:

$$U_T(\Omega) = \exp\left(-2\left(\frac{2\Omega}{\Omega_{ch}}\right)^2\right) = \exp\left(-2\eta^2\right) \tag{27}$$

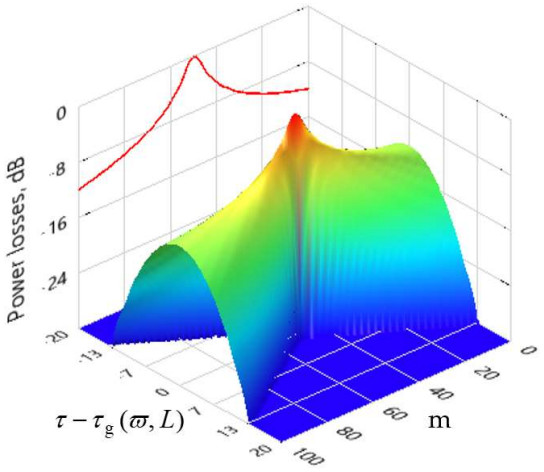

Figure 3. The computing results of the compression of line frequency-modulated pulse with the Gauss form in the fiber with second-order dispersion in dimensionless values. The effect reaches its maximum at communication link length $L = 50\cdot L_{e2}$, with 10 dB gain

The increase of the amplitude and the increase of the optical loss due to second-order dispersion have similar values (the curve is symmetrical about the maximum). To prevent second-order dispersion, methods of pre-distortion of a light pulse during transmission or correction of dispersion during reception are used. This effect illustrates a technique for overcoming second-order dispersion by transmitting an optimal chirp pulse to the channel.

With an increase in the length of the optical fiber, the third-order dispersion can be of fundamental importance. It can be shown that in this case, the analytical solution for the impulse response has the form:

$$h(\varpi,\tau,L) = \frac{H(\varpi,L)}{\sqrt[3]{\varphi'''(\varpi,L)/2}}\exp(j\varpi\tau)\cdot\left\{\mathrm{Ai}\left(-\frac{\tau-\tau_g(\varpi,L)}{\sqrt[3]{\varphi'''(\varpi,L)/2}}, -\frac{\Omega_{ch}}{4\pi}\right) - \mathrm{Ai}\left(-\frac{\tau-\tau_g(\varpi,L)}{\sqrt[3]{\varphi'''(\varpi,L)/2}}, \frac{\Omega_{ch}}{4\pi}\right)\right\} \tag{28}$$

where:

$$\mathrm{Ai}(u,t) = \frac{1}{2\pi}\int_t^{\infty}\exp\left(j\left(\frac{x^3}{3}+xu\right)\right)dx$$

are incomplete Airy integrals.

In the dimensionless variables the line length was chosen under conditions that a channel with third-order dispersion coherence bandwidth is equal to its frequency bandwidth

Preprints (www.preprints.org) | NOT PEER-REVIEWED | Posted: 8 December 2020 doi:10.20944/preprints202012.0192.v1

$\Omega_{C3} = \Omega_{ch} : L_{e3} = 6c/|(\varpi n(\varpi))'''|(\Omega_{ch}/2)^3$. In this case, the dimensionless communication line length is $m = L/L_{e3}$, the dimensionless dispersion coefficient is $p_{e3} = \Omega_{ch}/\Omega_{C3} = 1$, and dimensionless frequency is $\eta = 2\Omega/\Omega_{ch} \in [-1, 1]$. The third-order nonlinear component at given dimensionless values for phase equals:

$$\frac{1}{6}\varphi'''(\varpi, L)\cdot\Omega^3 = \left(\frac{L}{L_{e3}}\right)\cdot\left(\frac{2\Omega}{\Omega_{ch}}\right)^3 = m\cdot\eta^3 \tag{29}$$

It must be noted, that dimensionless length differs from the length, which was taken for second-order dispersion.

The results of calculating the Gaussian pulse distortion for TOD > 0 and TOD < 0 are shown in Figure 4,*a* and 4,*b*, respectively. In both cases, starting from a certain length of the optical path, the effect of pulse collapse is observed when it disintegrates into many short pulses. The number of additional pulses depends on the path length (the value of the TOD parameter). At TOD > 0, the collapse appears behind the main pulse and at TOD < 0 – in front of it. Obviously, the collapse is described by Airy integrals (28).

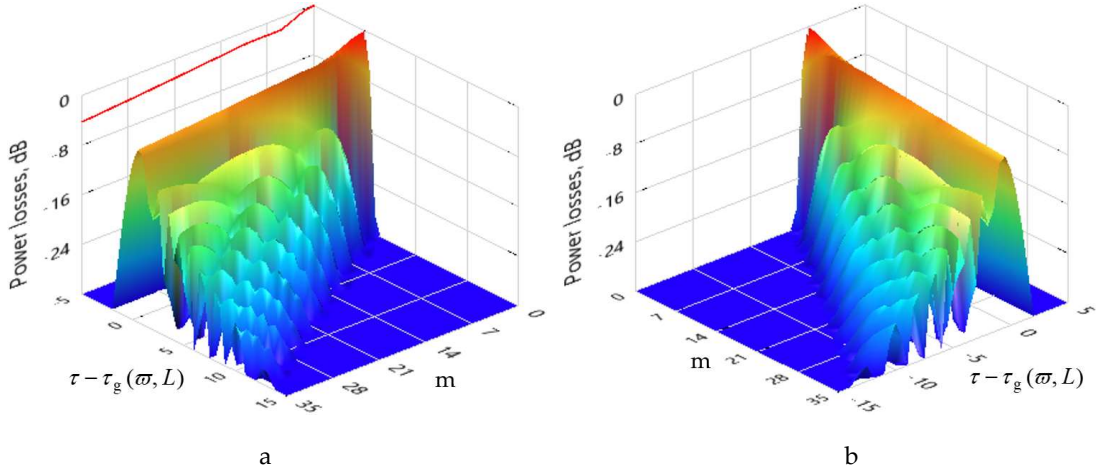

Figure 4. The short pulse collapse in fiber: a) *TOD* > 0; b) *TOD* < 0.

In the case of second- and third-order dispersion, as the line length increases, in the beginning the pulse broadening is observed, then its asymmetry appears, and then collapse occurs.

4. Conclusions

In our research we showed that the suggested method can be successfully used for solving the coupled nonlinear Schrödinger equation system in case of strongly coupled groups of modes for pulse evolution. In additional to the results given in [1], the separation of the nonlinear system of Schrödinger equations into set of independent linear equation systems at each integration step allows us to include an arbitrary number of propagation modes into equations and investigate their mutual influence. Results, received from model task investigations and their comparison with other researchers' results, as well as experimental data, allows us to conclude that the suggested method is effective, advantageous and has potential for future improvement.

Within the framework of the channel model, an analytical solution is obtained. It describes the propagation of an optical pulse in an optical fiber with a varying length. It is shown that the second-order frequency dispersion can lead to the effect of compression of the optical chirp pulse if the dispersion parameter GDD and the rate of change of the frequency ω′ differ in sign, and if their modules are inversely proportional, then the maximum compression takes place, i.e. such a pulse is optimal for a fiber of a given length. This effect can be used for optical pulse pre-distortion. The third-order dispersion increasing with length at the beginning leads to an asymmetry of a pulse with a Gaussian envelope, and then to a collapsing effect when it decays into many short adjacent pulses.

At TOD > 0, the collapse appears behind the main pulse, and at TOD < 0 – in front of it. In the case of second and third-order dispersion, as the cable length increases, in the beginning the pulse broadening is observed, then its asymmetry appears, and then collapse occurs.

Author Contributions: Conceptualization, A.Zh.S., D.V.I.; Formal analysis, V.I.A., D.V.I., V.A.I., and V.A.B.; Funding acquisition, O.G.M., A.V.B., M.I.R. and A.A.K.; Investigation, A.Zh.S., V.I.A., V.A.B., A.A.K., D.V.I., A.A.I., M.I.R. and I.M.G.; Methodology, A.Zh.S., V.I.A., O.G.M., and V.A.B.; Software, A.Zh.S. and V.I.A.; Supervision, V.A.B., and A.V.B.; Validation, A.Zh.S., V.I.A., O.G.M. and V.A.B.; Visualization, V.V.O., A.Zh.S.; Writing – review & editing, A.Zh.S.

Funding: Russian Foundation for Basic Research: 9-37-90057, President of the Russian Federation for state support of young Russian scientists – 347 candidates of sciences MK-3421.2019.8: 075-15-2019-309, Russian Foundation for Basic Research: 19-57-80006 346 BRICS_t, Russian Science Foundation: 18-19-00401.

Conflicts of Interest: The authors declare no conflict of interest.

References

1. Zhavdatovich Sakhabutdinov, A.; Ivanovich Anfinogentov, V.; Gennadievich Morozov, O.; Alexandrovich Burdin, V.; Vladimirovich Bourdine, A.; Mudarrisovich Gabdulkhakov, I.; Anatolievich Kuznetsov, A. Original Solution of Coupled Nonlinear Schrödinger Equations for Simulation of Ultrashort Optical Pulse Propagation in a Birefringent Fiber. *Fibers* 2020, *8*, 34.
2. Samad, R.; Courrol, L. Ultrashort Laser Pulses Applications, Coherence and Ultrashort Pulse Laser Emission; IntechOpen: UK, 2010; pp. 663–688. Ricardo Samad, Lilia Courrol, Sonia Baldochi and Nilson Vieira (December 30th 2010). Ultrashort Laser Pulses Applications, Coherence and Ultrashort Pulse Laser Emission, F. J. Duarte, IntechOpen, pp. 663–688, doi: 10.5772/13095.
3. Sugioka, K.; Cheng, Y. Ultrafast lasers—Reliable tools for advanced materials processing. *Light Sci. Appl.* **2014**, *3*, e149.
4. Sugioka, K. Progress in ultrafast laser processing and future prospects. *Nanophotonics* **2017**, *6*, 393–413, doi:10.1515/nanoph-2016-0004.
5. Hodgson, N.; Laha, M. *Industrial Femtosecond Lasers and Material Processing*; Industrial Laser Solutions, PennWell Publishing: Tulsa, OK, USA, 2019.
6. Göbel, W.; Nimmerjahn, A.; Helmchen, F. Distortion-free delivery of nanojoule femtosecond pulses from a Ti:sapphire laser through a hollow-core photonic crystal fiber. *Opt. Lett.* **2004**, *29*, 1285–1287, doi:10.1364/ol.29.001285.
7. Michieletto, M.; Lyngsø, J.K.; Jakobsen, C.; Lægsgaard, J.; Bang, O.; Alkeskjold, T.T. Hollow-core fibers for high power pulse delivery. *Opt. Express* **2016**, *24*, 7103–7119, doi:10.1364/oe.24.007103.
8. Karasawa, N.; Nakamura, S.; Morita, R.; Shigekawa, H.; Yamashita, M. Comparison between theory and experiment of nonlinear propagation for 4.5-cycle optical pulses in a fused-silica fiber. *Nonlinear Opt*. **2000**, *24*, 133–138.
9. Nakamura, S.; Li, L.; Karasawa, N.; Morita, R.; Shigekawa, H.; Yamashita, M. Measurements of third-order dispersion effects for generation of high-repetition-rate, sub-three-cycle transform-limited pulses from a glass fiber. *Jpn. J. Appl. Phys.* **2002**, *41*, 1369–1373, doi:10.1143/jjap.41.1369.
10. Nakamura, S.; Koyamada, Y.; Yoshida, N.; Karasawa, N.; Sone, H.; Ohtani, M.; Mizuta, Y.; Morita, R.; Shigekawa, H.; Yamashita, M. Finite-difference time-domain calculation with all parameters of Sellmeier's fitting equation for 12-fs laser pulse propagation in a silica fiber. *IEEE Photon. Technol. Lett.* **2002**, *14*, 480–482, doi:10.1109/68.992584.
11. Nakamura, S.; Takasawa, N.; Koyamada, Y. Comparison between finite-difference time-domain calculation with all parameters of Sellmeier's fitting equation and experimental results for slightly chirped 12-fs laser pulse propagation in a silica fiber. *J. Light. Technol.* **2005**, *23*, 855–863, doi:10.1109/JLT.2004.838873.
12. Nakamura, S.; Takasawa, N.; Koyamada, Y.; Sone, H.; Xu, L.; Morita, R.; Yamashita, M. Extended finite difference time domain analysis of induced phase modulation and four-wave mixing between two-color femtosecond laser pulses in a silica fiber with different initial delays. *Jpn. J. Appl. Phys.* **2005**, *44*, 7453–7459, doi:10.1143/jjap.44.7453.
13. Nakamura, S. Comparison between finite-difference time-domain method and experimental results for femtosecond laser pulse propagation. *Coherence Ultrashort Pulse Laser Emiss.* **2010**, 442–449, doi:10.5772/12854.

14. Burdin, V.A.; Bourdine, A.V. Simulation results of optical pulse non-linear few-mode propagation over optical fiber. *Appl. Photon*. **2016**, *3*, 309–320. (In Russian)
15. Burdin, V.A.; Bourdine, A.V. Model for a few-mode nonlinear propagation of optical pulse in multimode optical fiber. In Proceedings of the OWTNM, Warsaw, Poland, 20–21 May 2016.
16. Sakhabutdinov, A.Z.; Anfinogentov, V.I.; Morozov, O.G.; Gubaidullin, R.R. Numerical approaches to solving a nonlinear system of Schrödinger equations for wave propagation in an optical fiber. *Comput. Technol*. **2020**, *25*, 42–54, doi:10.25743/ICT.2019.24.1.004.
17. Ivanov, V. A.; Ivanov, D. V.; Ryabova, N. V.; Ryabova, M. I.; Chernov, A. A.; Ovchinnikov; V. V. Studying the parameters of frequency dispersion for radio links of different length using software-defined radio based sounding system. *Radio Sci.*, **2019**, *54*, 34–43. doi:10.1029/2018RS006636.
18. Agrawal, G. P. *Nonlinear Fiber Optics (fourth edition)*. Academic Press: San Diego, CA, USA, 2006.
19. Xiao, Y.; Maywar, D.N.; Agrawal, G.P. New approach to pulse propagation in nonlinear dispersive optical media. *J. Opt. Soc. Am. B*, **2012**, vol. 29, no. 10, 2958-2963.
20. Ivanov, D.V. Methods and mathematical models for studying propagation of spread spectrum signals in the ionosphere and correction for their dispersion distortions: monograph. MarSTU: Yoshkar-Ola, 2006, 268p. (In Russian)